

On the incipient breaking of small scale waves

By M. L. BANNER AND O. M. PHILLIPS

Department of Earth and Planetary Sciences,
The Johns Hopkins University, Baltimore, Maryland 21218

(Received 21 June 1973 and in revised form 10 January 1974)

It is shown that the surface wind drift in the ocean substantially reduces the maximum wave height ζ_{\max} and wave orbital velocity that can be attained before breaking. If q is the magnitude of the surface drift at the point where the wave profile crosses the mean water level and c is the wave speed, then

$$\zeta_{\max} = \frac{c^2}{2g} \left(1 - \frac{q}{c}\right)^2.$$

Incipient breaking in a steady wave train is characterized by the occurrence of stagnation points at wave crests, but not necessarily by discontinuities in slope. After breaking, there is in the mean flow a stagnation point relative to the wave profile near the crest of the broken wave, on one side of which the water tumbles forward and behind which it recedes more smoothly to the rear. Some simple flow visualization studies indicate the general extent of the wake behind the breaking region.

1. Introduction

The breaking of wind-generated waves is a widespread but little understood phenomenon in the open ocean. In a recent paper, Longuet-Higgins (1973) remarks that “our knowledge of breaking waves is surprisingly scanty” and, indeed, prior to his paper little, if any, work had been done on the detailed dynamics of breaking waves. The reason lies not in a lack of awareness of the importance of breaking waves, but in the difficulty of making detailed measurements of a transient phenomenon and in the analytical difficulty presented by an intrinsically unsteady, vortical free-surface flow. There is considerable observational data concerned with the structure of breakers on shoaling beaches where the whole wave collapses in shallow water into something akin to a bore or hydraulic jump, but in deep water the breaking is more sporadic and fugitive, developing fairly abruptly, persisting for a time and then subsiding as the wave crest passes on. The process of breaking seems to involve the formation of a region at the wave crest that spills forward forming a necessarily turbulent region on the forward face and leaving behind a less turbulent wake that decays with increasing distance from the wave crest. If the turbulent motion in the breaking region becomes sufficiently intense, air entrainment occurs and visible ‘whitecaps’ are formed, but the occurrence of breaking itself seems to be far more widespread than the occurrence of whitecaps.

Figure 1 (plate 1) is a photograph, taken from above, of the crest of a small scale breaking wave in our wind-wave tunnel at The Johns Hopkins University. Mechanically generated waves with a maximum slope of 0.29 were produced at the upwind end of the tank and the photograph was taken at a fetch of 10.36 m with a surface wind stress of $1.6 \text{ dynes cm}^{-2}$. The broken region, advancing to the right, is clearly turbulent though entraining very little air and is characterized by an irregular steep leading face where the water is tumbling forward in irregular and rapidly changing fingers. The motion is highly unsteady in detail though the breaking zone persists for some time. Figure 2 (plate 2) shows what appear to be similar structures observed in the field by Mr Mart Peep in a photograph taken from the *R. V. Ridgely Warfield* in the Chesapeake Bay. The wind is blowing at about 15 knots from the upper left-hand corner of the photograph to the middle right and the crest of a long wave lies diagonally across the photograph near the upper left. Over the forward face of the long wave is a dense structure of wavelets with the irregular steep leading edges characterizing small scale breaking, though again without air entrainment. The spatial separation of the steps varies up to about 20 cm. This kind of 'micro-breaking' can, with a quick eye, be seen to be quite widespread under ocean conditions in an active wind field and is, of course, of central importance in the transfer of energy and momentum from the wave field to near-surface turbulence and wind-generated currents. It also provides for greatly augmented transfer of heat and dissolved gases across the air-sea interface.

The limiting form of steady irrotational gravity waves is one with sharp crests containing an angle of 120° (Stokes 1880; Michell 1893) but it is very difficult, even in the laboratory, to generate a wave train that approaches this configuration. Quite apart from the instability of a train of finite amplitude surface waves (Benjamin & Feir 1967) the waves tend to become very unsteady as the curvature at the crest increases, so that even a small perturbation results in breaking. At sea, under the action of the wind, waves are neither steady nor irrotational (because of the surface shear stress, if nothing else), so that the existence of the Stokes limit is hardly a useful one. Nevertheless, it is of interest to point out that the sharp crest coincides with a stagnation point in the flow when observed in a frame of reference moving with the wave. We show below that it is the presence of a stagnation point on the surface that is an essential part of wave breaking rather than the formation of a sharp crest, and that the surface drift induced by the wind has a substantial influence on the occurrence of such stagnation points.

The spirit of this paper is rather different from that of Longuet-Higgins (1973). He assumed that the free surface of the forward spilling region is fixed in time and was concerned with the dynamical properties of the stagnation-point flow formed by the oncoming (irrotational) motion, the spilling region (assumed to be steady but with an eddy viscosity representing the effects of turbulence), and the air flow above the free surface. We, on the other hand, will examine the conditions under which breaking is incipient in the presence of a wind drift and some simple properties of the flow once breaking has occurred. Valuable guidance is given by observation and measurement in both the wind-wave tank

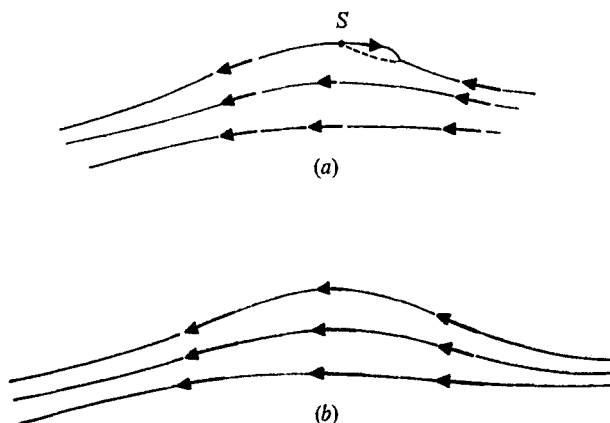


FIGURE 3. The occurrence of a stagnation point S near the crest of a breaking wave, ahead of which water is tumbling forward.

and a laboratory flume. Our object is to combine these observations with a partial but simple theoretical analysis to adduce some of the salient characteristics of the breaking process.

2. The onset of breaking

A breaking wave can be defined as one in which certain fluid elements at the free surface (near the wave crest) are moving forward at a speed greater than the propagation speed of the wave profile as a whole. When a wave breaks on a sloping beach, the fluid may plunge forward enclosing an air bubble (a cylinder of air in a two-dimensional motion) or it may spill. In deep water, the spilling motion is much more characteristic, with the fluid elements sliding down the leading slope. At larger scales of breaking, air entrainment may take place and the breaking wave is clearly visible as a whitecap, but as we have pointed out, air entrainment is not a necessary concomitant to wave breaking. If the motion is viewed in a frame of reference moving with the wave profile, as in figure 3 (a), the general motion of the fluid elements is to the left, while near the wave crest, fluid is on average moving to the right. The motion in the spilling region is necessarily turbulent and the position of the free surface unsteady with respect to the general profile, but the reversal in the direction of the mean flow at the surface requires the existence of a stagnation point in the mean flow, indicated by the point S .

In an unbroken wave, observed in the same frame of reference, the fluid elements are all moving to the left. Since the pressure on the free surface of a gravity wave is, in essence, constant, fluid elements of the surface approaching the wave crest decrease in speed as their elevation increases. With increasing wave elevation, the speed with which they arrive at the crest decreases and the point of incipient breaking is reached when this speed drops to zero and the fluid elements may either continue on the left, or reverse direction and spill forward to the right. If the motion is irrotational, this occurs when the surface has attained the Stokes limiting form with a sharp crest, but if the flow is rotational there is

no necessity for the stagnation point at the wave crest to be associated with a discontinuity in surface slope.

In the ocean, the mean tangential stress of the wind and the momentum loss from short capillary waves as a result of their viscous dissipation both contribute to the surface wind drift, whose magnitude is of the order 3% or 4% of the mean wind speed as usually measured at a height of 10 m. A similar value is found in wind-wave tunnels, Wu (1968) measuring a surface drift of about 4% of the mean velocity in the tunnel. The shear (and so the vorticity) at the surface is very large since the turbulent Reynolds stresses in the water are negligible at the surface and the tangential wind stress must be supported entirely by molecular viscosity. The thickness of this high shear region is, however, very small, as it is in the viscous sublayer adjacent to a rigid wall, since, with increasing depth, the turbulent Reynolds stresses very soon dominate the molecular viscous stress supported by the mean shear, and the velocity gradient decreases abruptly. The thickness of this surface wind-drift (viscous) layer must be proportional to $\nu(\rho_w/\tau_s)^{1/2}$, where ν is the molecular viscosity of the water, with density ρ_w , and τ_s is the mean tangential wind stress. In the laboratory, Wu measured thicknesses of 3–5 mm; those in the ocean are likely to be of the same order at moderate wind speeds.

The presence of this layer has little effect on the phase speed or subsurface orbital velocities of gravity waves whose wavelength is very much larger than the layer depth. It does, however, significantly modify the propagation of short capillary waves but, even more, it enhances the formation of stagnation points at the crests of short gravity waves and consequently the occurrence of incipient breaking. This can be seen qualitatively from figure 3(b). If the wind is blowing to the right (in the same direction as the waves travel) then the surface drift is in this direction also, subtracting from the speeds indicated. A fluid element at the surface in a wave trough has less kinetic energy to be converted to potential energy as it rides over the wave crest, so that the maximum elevation it can attain before its speed drops to zero is likewise reduced.

More precisely, let us suppose that, in an unbroken wave, the motion is steady in a frame of reference moving with the wave profile. The tangential wind stress is responsible for the layer of large vorticity near the surface, but the response time of the layer to variations in wind stress can be supposed large compared with a wave period. Accordingly, we can assume that the surface layer is established by viscous action over a time scale much greater than the time it takes a fluid element to move from crest to trough, and over these times the influence of molecular viscosity on the already vortical fluid can be neglected. The equation of motion can be written in the form

$$\mathbf{u} \times \boldsymbol{\omega} = -\nabla(\frac{1}{2}u^2 + gz + p/\rho). \quad (2.1)$$

At the surface $z = \zeta$, the pressure can be assumed constant and the velocity vector \mathbf{u} and the vorticity vector $\boldsymbol{\omega}$ both lie in the surface, so that $\mathbf{u} \times \boldsymbol{\omega}$ is in the direction of the normal. The tangential component of (2.1) is therefore

$$\partial(\frac{1}{2}u_s^2 + g\zeta)/\partial s = 0, \quad (2.2)$$

where s is measured along the surface. Consequently

$$\begin{aligned} \frac{1}{2}u_s^2 + g\zeta &= \text{constant} \\ &= \frac{1}{2}u_s^2(0), \end{aligned} \tag{2.3}$$

where $u_s(0)$ represents the surface speed at the point where $\zeta = 0$, where the profile intersects the mean surface level. The surface speed is therefore least when the surface elevation is greatest, and a stagnation point will arise first at a wave crest when

$$\zeta = \zeta_{\max} = u_s^2(0)/2g. \tag{2.4}$$

The greater the mean wind drift in the direction of wave propagation, the smaller the u_s^2 observed in this frame of reference and the smaller the surface elevation required to produce stagnation.

The surface speed u_s is the resultant of the orbital velocity of the wave motion referred to rest, the velocity $-c$ of a rest origin in the frame of reference moving with the wave, together with the surface wind drift. The last of these is not independent of the orbital velocity in the wave, since the surface straining tends to bunch the vortex lines in the surface layer at regions of maximum convergence at the wave crests. This has the effect of locally increasing the surface drift at the crest above the average value for the whole surface, and further reducing the resultant speed at the crest, as can be demonstrated by the following simple analysis.

Consider a locally orthogonal co-ordinate system in which $\eta = 0$ represents the surface of the unbroken wave and s is the distance along the surface from a suitable origin. We are interested only in the region of space occupied by the wind-drift layer, whose depth is very much less than the wavelength of the wave; over this range the orbital velocity of the wave is substantially constant and the co-ordinates are locally Cartesian. The tangential velocity component can be expressed as

$$u = U(\epsilon s) + u_d(\epsilon s, \eta), \tag{2.5}$$

where the irrotational part U represents the combined orbital velocity and the velocity $-c$ in the x direction of a fixed origin with respect to the moving frame, and u_d is the surface drift velocity. The ratio ϵ^{-1} of the scales of variation of the velocity in the s direction and in the η direction is the ratio of the wavelength to the depth of the wind-drift layer, so that $\epsilon \ll 1$. The normal component of the velocity field, by continuity, is

$$v = -\epsilon\eta U'(\epsilon s) + v_d(\epsilon s, \eta) \tag{2.6}$$

since both v and v_d vanish at $\eta = 0$. U is irrotational and the vorticity expressed in the orthogonal (η, s) co-ordinates in a two-dimensional motion can be shown (Longuet-Higgins 1960, p. 294) to be

$$\omega = -\frac{\partial u_d}{\partial \eta} \{1 + O(\epsilon)\} \simeq -\frac{\partial u_d}{\partial \eta}. \tag{2.7}$$

The vorticity equation

$$u \partial \omega / \partial s + v \partial \omega / \partial \eta = 0$$

can therefore be expressed, invoking the incompressibility condition again, as

$$\frac{\partial}{\partial s} \left\{ u \frac{\partial u_d}{\partial \eta} \right\} + \frac{\partial}{\partial \eta} \left\{ v \frac{\partial u_d}{\partial \eta} \right\} = 0,$$

which can be integrated from a depth $\eta = -\delta$ just below the vortical layer to the surface $\eta = 0$.

$$\frac{\partial}{\partial s} \int_{-\delta}^0 u \frac{\partial u_d}{\partial \eta} d\eta = - \left[v \frac{\partial u_d}{\partial \eta} \right]_{-\delta}^0 = 0,$$

since, at $\eta = 0$, $v = 0$ and, at $\eta = -\delta$, the vorticity $\partial u_d / \partial \eta = 0$. Thus the total vorticity flux

$$\int_{-\delta}^0 u \frac{\partial u_d}{\partial \eta} d\eta = \text{constant along the surface.}$$

But in the surface layer, $u = U + u_d$, and over this range of η , U is independent of η (to order ϵ), so that

$$\begin{aligned} \int_{-\delta}^0 u \frac{\partial u_d}{\partial \eta} d\eta &= \int_{-\delta}^0 (U + u_d) \frac{\partial}{\partial \eta} (U + u_d) d\eta \\ &= \frac{1}{2} [U(s) + u_d(s, 0)]^2 - \frac{1}{2} U^2(s) \\ &= \frac{1}{2} B, \text{ say, a constant,} \end{aligned}$$

where $u_d(s, 0)$ is the value of the tangential drift at the surface. Consequently

$$u_d^2(s, 0) + 2U(s)u_d(s, 0) - B = 0 \quad (2.8)$$

and

$$u_d(s, 0) = -U(s) \pm \{U^2(s) + B\}^{\frac{1}{2}}. \quad (2.9)$$

The tangential surface speed is therefore

$$\begin{aligned} u_s &= U(s) + u_d(s, 0) \\ &= -\{U^2(s) + B\}^{\frac{1}{2}}, \end{aligned} \quad (2.10)$$

the negative sign being taken in virtue of the direction of the flow shown in figure 3(b).

Now, in a purely irrotational motion, the surface velocity at the point where the wave profile crosses the mean water level is precisely equal to c , the wave speed, according to an old result of Levi-Civita (see Lamb 1953, p. 420). The proof given by Lamb carries through exactly for the irrotational part of the flow but the interpretation is slightly different: at the point where the bounding streamline of the irrotational region (just below the surface layer) crosses the mean level of this streamline, the water speed is exactly equal to c . If the surface layer is thin compared with the length of the wave, the horizontal location of this point closely approximates the point where the free surface crosses its own mean level and, if the superimposed drift at this point is q , then $u_d = q$ and $U = -c$ at this point and from (2.8)

$$B = -q(2c - q).$$

Consequently, from (2.10),

$$u_s = -\{U^2(s) - q(2c - q)\}^{\frac{1}{2}}. \quad (2.11)$$

If breaking is not to occur, the quantity in curly brackets must remain positive. At a wave crest, the surface is horizontal, so that $U = -c + U_0$, where U_0 is the

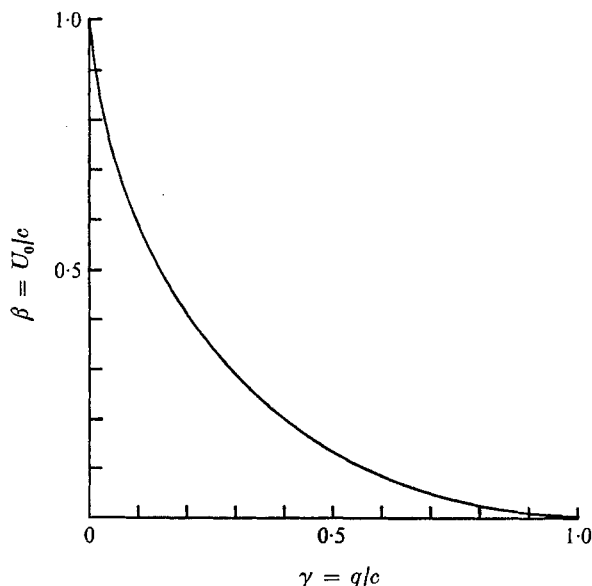


FIGURE 4. The maximum orbital velocity at the wave crest U_0 that can be attained without wave breaking, as a function of the surface drift q at the mean water level $\zeta = 0$.

maximum forward orbital velocity in the irrotational part of the wave, so that the surface velocity there is

$$(u_s)_{\text{crest}} = -\{(c - U_0)^2 - q(2c - q)\}^{\frac{1}{2}}, \quad (2.12)$$

and the condition that breaking should not occur is that

$$\begin{aligned} (c - U_0)^2 &> q(2c - q), \\ (1 - \beta)^2 &> \gamma(2 - \gamma), \end{aligned} \quad (2.13)$$

where $\beta = U_0/c$, the ratio of the maximum forward orbital speed in the irrotational part of the wave to the wave speed, and $\gamma = q/c$, the ratio of the surface drift at the mean level to the wave speed. This condition is illustrated in figure 4.

The maximum height that the wave can attain without breaking is found immediately from (2.3). The surface speed at the point where $\zeta = 0$ is, as was mentioned above, $-c + q$, so that

$$\zeta_{\text{max}} = \frac{(c - q)^2}{2g} = \frac{c^2}{2g}(1 - \gamma)^2. \quad (2.14)$$

The substantial influence of wind drift in limiting the maximum height that waves can attain before the occurrence of a stagnation point and a breaking region is immediately evident from these expressions. In the Stokes limiting irrotational wave without wind drift, $\gamma = 0$, $\zeta = c^2/2g$ and $\beta = 1$; the orbital velocity at the sharp wave crest is just equal to the wave speed. As γ increases, however, the maximum wave height and the forward irrotational orbital velocity at the wave crest both decrease rapidly. For example, in a 20 knot wind, the mean velocity at a height of 10 m is about 10 m/s, and the mean surface wind drift is approximately 30 cm/s. If q is taken as 30 cm/s, then a wavelet with wavelength

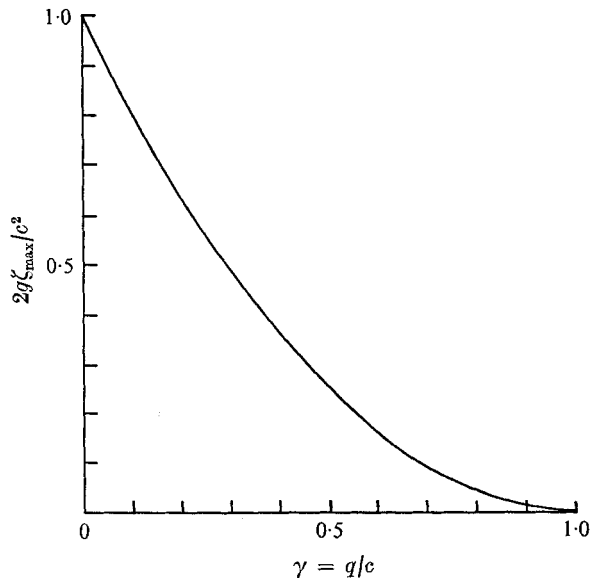


FIGURE 5. The maximum elevation ζ_{\max} above mean water level that can be attained without wave breaking, as a function of the surface drift q at $\zeta = 0$.

30 cm has a speed of 68 cm/s, so that $\gamma = 0.44$. The maximum unbroken wave height, from (2.14) or figure 5, is only 0.31 times the Stokes limit for irrotational waves, and the irrotational orbital speed at the wave crest is only 0.17c at the onset of breaking.

If short wavelets are riding over longer waves as in the photograph of figure 2 (plate 2), the surface wind drift near the crest of the longer wave is augmented by the large scale convergence. Short waves in these regions then experience a locally averaged wind drift that is greater than in other regions, so that the maximum height above the local mean surface that they can have without breaking is further reduced.

3. Some observations of the flow in a wave that is just breaking

In the wind-wave tank, the continuous observation of a breaking wave is difficult because of the fugitive nature of the phenomenon. For this reason, we decided to generate a standing breaking wave in a small flume across which air could be drawn to provide a surface stress.

The working section of our glass-sided flume is approximately 30 cm high and 15 cm wide; it was roofed over and a fan installed to draw air over the water surface. The standing wave was generated by a horizontal bar placed laterally across the flume a few centimetres above the floor of the inlet to the working section, and by adjustment of the height of the bar, the speed of flow and the fan speed, a standing breaking wave could be established and maintained as a statistically steady motion. The water depth was sufficiently great that the influence of the bottom was unimportant for the breaking region.

Flow visualization was achieved in two ways. A sheet of hydrogen bubbles

was generated by electrolysis from a vertical wire upstream of the breaking region and photographs (of which figure 6, plate 3, is typical) were taken by Mr J. Duncan with a high-speed ($50\mu\text{s}$) electronic strobe. Figure 7 (plate 3) identifies some aspects of the photograph. It was taken from a viewpoint slightly below the water level and the diffuse light line at the top represents the meniscus at the water surface at the near side of the tank. The free surface at the plane of the hydrogen bubbles is below this; the fuzzy dots representing reflexions of the illuminated bubbles from the underside of the free surface. Near the bottom, the flow is highly turbulent in the wake of the bar that produced the wave, but the region of laminar flow above this is evident. The interesting part of the photograph is the turbulent wake trailing behind the breaking region and extending beyond the field of view to the right. The turbulent intensity in this wake is not great but the disappearance of the streamlines in the laminar flow into the turbulence gives some evidence of active entrainment. From this and similar photographs, it appears that, in this region, the depth of the turbulent wake generated by breaking was of the order of the height of the breaking zone, though it was not possible to determine whether or not this is universally true because of the relatively small range of variations possible in this flume.

Complementary information was obtained by streak photographs (not shown) in which small residual air bubbles provided convenient markers. In the region occupied by the wake of the breaking zone, the streaks were all aligned close to the direction of mean flow, indicating that the turbulent intensity is small compared with the wave speed. Beyond this fact, it was not possible to estimate the magnitude of the turbulent velocity fluctuations in this way. The region of low velocity relative to the wave crest was confined to the crest itself and the tumbling part immediately in front of it, suggesting strongly that the rolling eddy at the breaking front occupies only this region with a mean stagnation point where the flow diverges near the wave crest where the surface slope vanishes.

Fingers of water, tumbling forward, encounter the oncoming stream at a point that varies erratically in time. Unlike the model proposed by Longuet-Higgins (1973) the experimental flow has no fixed forward stagnation point. If the mean flow is considered, the definite location of the free surface in the breaking eddy disappears and must be replaced by an intermittent zone in which each fixed point is beneath the water surface for only a fraction of the total averaging time.

It would clearly be very desirable to make careful measurements of the surface velocity and wave height when the wave is still unbroken but as close as possible to the point of incipient breaking in order to compare the results with equation (2.13) and figure 4. The degree of control available on the small flume used here was such that it was not possible to maintain the wave just at the point of incipient breaking long enough for measurements to be made, though stable unbroken and broken waves could be generated easily. We hope that further measurements can be done with another facility.

This work was supported by the Office of Naval Research under Contract N00014-67A-0163-0009 for M. L. Banner and by the National Science Foundation under Grant GA-3539OX for O. M. Phillips.

REFERENCES

- BENJAMIN, T. B. & FEIR, J. E. 1967 The disintegration of wave trains on deep water. Part 1. Theory. *J. Fluid Mech.* **27**, 417.
- LONGUET-HIGGINS, M. S. 1960 Mass transport in the boundary layer at a free oscillating surface. *J. Fluid Mech.* **8**, 293.
- LONGUET-HIGGINS, M. S. 1973 A model of flow separation at a free surface. *J. Fluid Mech.* **57**, 129.
- LAMB, H. 1953 *Hydrodynamics*. Cambridge University Press.
- MICHELL, A. G. M. 1893 The highest waves in water. *Phil. Mag.* **36** (5), 430.
- STOKES, G. G. 1880 On the theory of oscillatory waves. *Papers*, pp. 1, 197, 227. Cambridge University Press.
- WU, J. 1968 Laboratory studies of wind-wave interactions. *J. Fluid Mech.* **34**, 91.

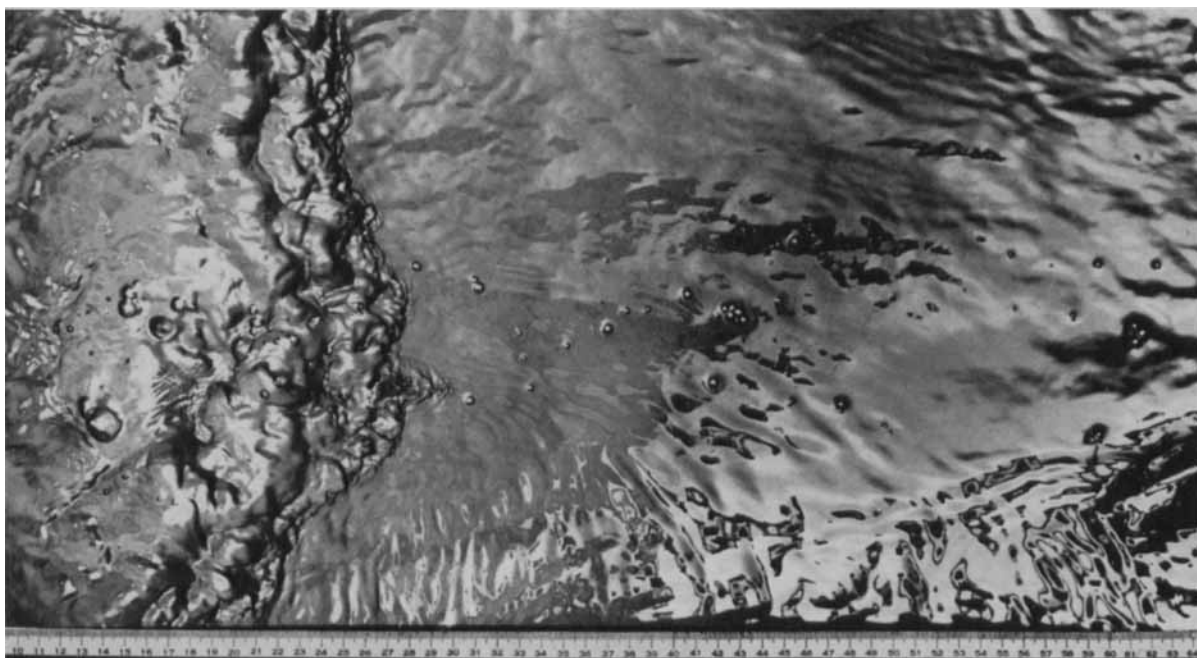


FIGURE 1. A breaking wave in the laboratory, viewed from above.

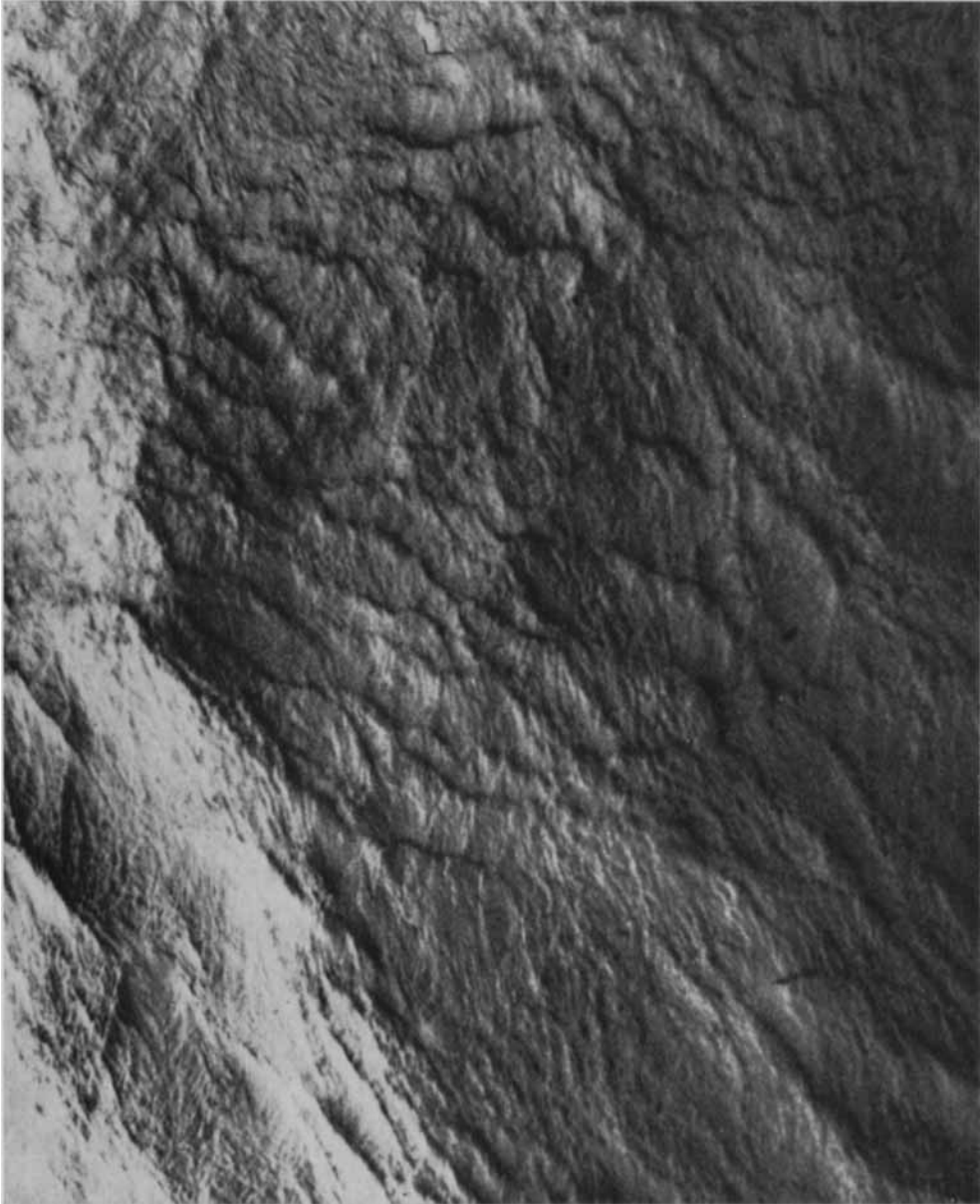


FIGURE 2. Small scale breaking wavelets in the field. Note the series of small steps (breaking fronts) on the forward slope of the longer wave in an active wind-generated field. No entrainment of air bubbles is apparent. Photograph by Mr Mart Peep.

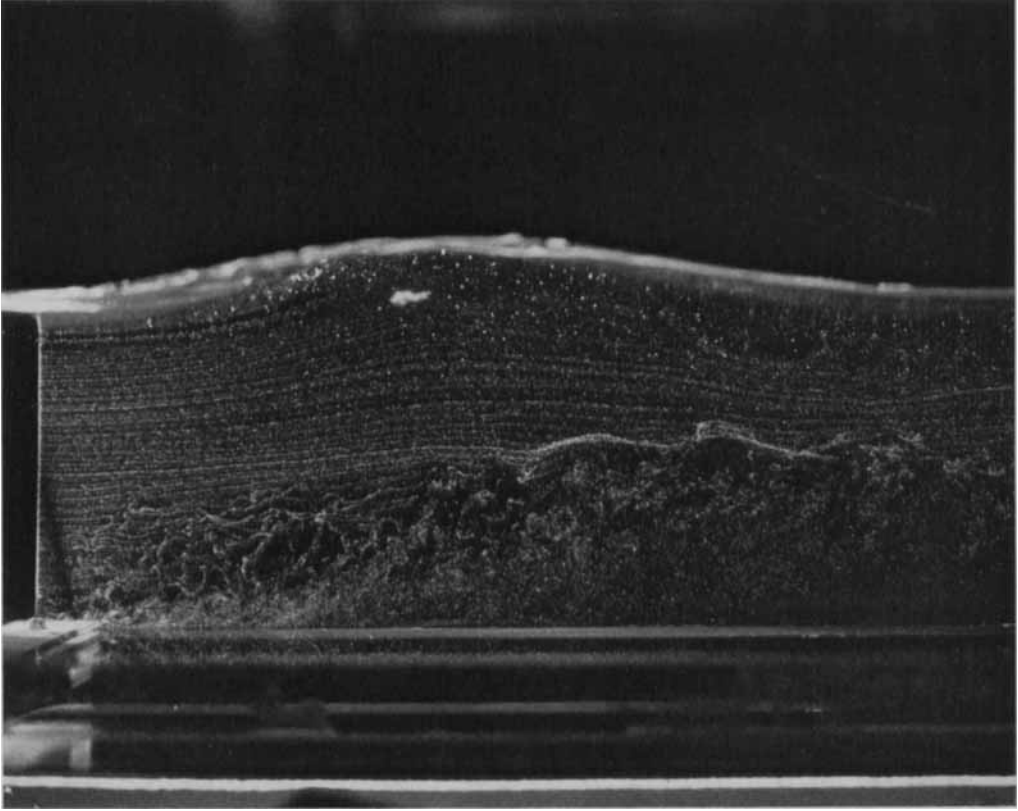


FIGURE 6. Streak lines in a small scale breaking wave. For identification, see figure 7.

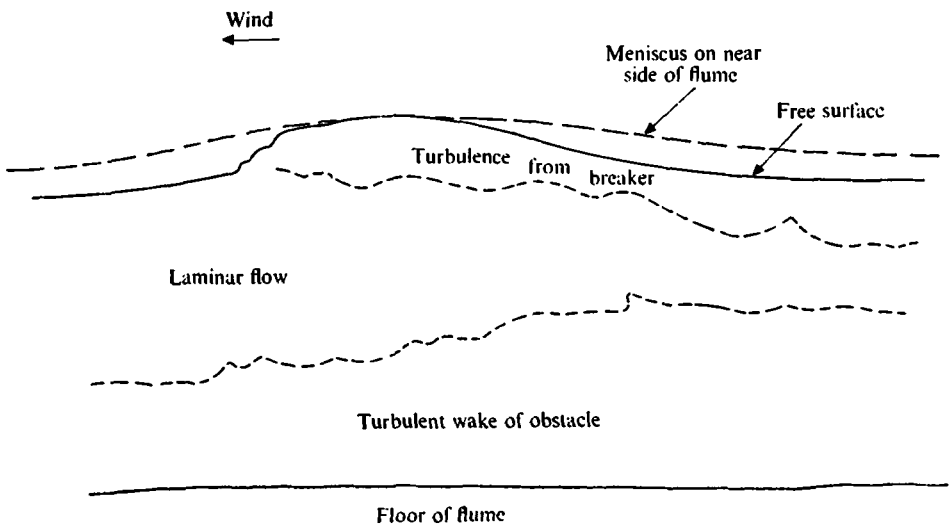


FIGURE 7. An identification of figure 6. The undisturbed water depth is 15 cm.

BANNER AND PHILLIPS